Chemical Papers (2025) 79:3097–3106
https://doi.org/10.1007/s11696-025-03990-0

ORIGINAL PAPER

Synthesis and physicochemical characterization of lanthanide complexes coordinated with spiropyran derivatives

Jorge Fernandes Z. Netto[1] · Flávio B. Miguez[1] · Nathália E. N. Mendonça[1] · Olívia B. O. Moreira[2] · Marcone A. L. de Oliveira[2] · Luiz F. C. de Oliveira[3] · Roberto S. Nobuyasu[4] · Frederico B. De Sousa[1]

Received: 30 November 2024 / Accepted: 25 February 2025 / Published online: 12 March 2025

Abstract

Among many molecules, spiropyran derivatives are still a target of interest for various research fields due to the distinctive physicochemical properties of their isomers in response to a variety of triggers, including light irradiation and solvent–solute interaction. Herein, 14 coordination complexes (LnMC) using the lanthanide ion series (from La^{3+} to Lu^{3+}, excluding the Pm ion) were coordinated with a spiropyran derivative (SPCOOH—l-(b-carboxyethyl)-3′,3′-dimethyl-6-nitrospiro(indoline-2′,2[2H-1]benzopyran). The ligand binding to these metal ions was achieved in organic solvent solution, using UV radiation to precipitate the complex. These complexes were characterized using electronic and spectrometric techniques, revealing that more than one structure can be obtained for the same metal ion by coordinating two or three SPCOOH in the lanthanide ion. The photochromic properties of these complexes were evaluated using electronic spectroscopy, with absorption maxima wavelengths ranging from 463 to 479 nm. The emission results showed no significant wavelength variation for most of the ions (ranging from 560 to 578 nm), suggesting that data emission is primarily dependent on the merocyanine isomer. The solvatochromic data exhibited a strong linear correlation for these LnMC complexes using 1-propanol, compared to other alcohols tested.

Graphical abstract

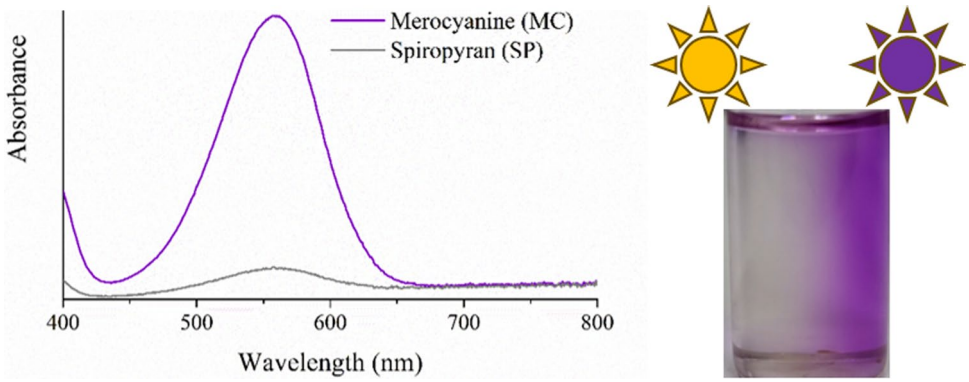

Keywords Coordination complex · Photochromism · Alcohols · Spiropyran · Solvatochromism

Extended author information available on the last page of the article

Introduction

Recently, there has been a growing interest in chromic phenomena, driven by the remarkable ability of materials to undergo color transformation in response to various stimuli. This phenomenon comprises a significant alteration in the molecular structure of the molecules involved, thereby exerting a considerable influence on their optical characteristics (Klajn 2014). Solvatochromism is gaining prominence among various stimuli to which molecules can be exposed, allowing to understand their electronic structure and molecular interactions with different environments resulting in a variation of colors (Homocianu 2024). This phenomenon is influenced by solvent properties such as polarity and solvation energy, which are crucial in eliciting diverse responses from chromic molecules (Danylchuk et al. 2021; Kortekaas and Browne 2019; Morimoto et al. 2018; Pandey et al. 2022; Stock et al. 2015). The polarity of the solvent influences the electron density distribution within the molecule, directly impacting the energy gap between the molecular orbitals of the ground and excited states involved in the electronic transition. Additionally, solvation energy can affect the complexation process, significantly influencing the ratio of the complex to free MC in solution. This, in turn, contributes to the color change, albeit through a different mechanism (Danylchuk et al. 2021). Among the different molecules capable of being responsive to the solvent medium spiropyrans stand out (Hur and Shin 2015; Liu et al. 2022; Miguez et al. 2019; Wang et al. 2023; Zhang et al. 2009).

Spiropyrans are a category of organic compounds distinguished by their ability to undergo a reversible isomerization process. This transformation occurs between two thermodynamically stable isomers, the spiro form (SP), which is non-planar and usually colorless in solution with a closed-ring structure, and the merocyanine (MC), an open-ring planar isomer characterized by its vivid coloration and due to its conjugated p system (Kortekaas and Browne 2019; Kozlenko et al. 2023; Menzonatto and Lopes 2022). As previously mentioned, spiropyrans molecules present solvatochromic properties, which have been detailed in a few research studies. Tian and colleagues also studied the solvatochromic phenomenon in 2014 (Tian and Tian 2014). In their study, the solvatochromic effect was analyzed using spiropyrans while employing the Hansen solubility parameters, which account for the energy of intermolecular forces, dispersion, and hydrogen bonding. It was demonstrated that the factors predominantly influencing the variation in maximum wavelength (λ_{max}) are solvent polarity and hydrogen bonding interactions; while the dispersion forces play a more significant role in determining absorbance variations (whether they increase or decrease) due to the solvation of the MC isomer. Abdollahi and coworkers demonstrated the solvatochromic behavior of a hydroxyl-functionalized spiropyran derivative (SPOH) by analyzing its interactions with various solvents and how the λ_{max} values are correlated with the intrinsic properties of the solvents (protic and aprotic) (Abdollahi et al. 2017). This was accomplished by employing the Hansen solubility parameters, as well as the Reichardt polarity scale. The study revealed that in aprotic environments, solvatochromism shows a strong dependence on the Hansen parameters, whereas in protic environments, there is a significant reliance on polarity. Further studies by Florea and coworkers applied spiropyran-polymer brushes for the functionalization of fused silica microcapillaries through surface-initiated ring-opening metathesis polymerization (Florea et al. 2013). Owing to the solvatochromic properties of these functionalized capillaries, they were successfully employed for the photo-identification of solvents with varying polarities as they flowed continuously through the microcapillary under UV irradiation (365 nm).

During the isomerization process, a phenolic group forms on the MC molecule, which increases its affinity to interact with metal ions, such as lanthanides (Abdel-Mottaleb et al. 2018; Attia et al. 2006; Reis et al. 2020; Gao et al. 2020; Netto et al. 2024; Selvanathan et al. 2016). Due to their unique properties, for example, luminescence, lanthanides have been applied in the formulation of lasers, and amplifiers for communication (Rocha et al. 2011). They also have medical applications, with elements like gadolinium, dysprosium, terbium, and europium being used as contrast agents in NMR analysis (Chen et al. 2014). Unlike d-block metals, lanthanides can support high coordination numbers, and the formation of coordination complexes offers benefits such as increased light absorption of the molecule (Bao et al. 2021), which can lead to unique characteristics and changes when exposed to different solvents, particularly when spiropyrans are used as ligands.

The study of solvatochromic properties in lanthanide complexes coordinated with spiropyran derivatives offers significant insights into the fundamental electronic interactions within these systems. Lanthanides, with their unique f-orbital characteristics, display intriguing photophysical properties that are highly sensitive to their environment. Coupling these properties with the well-known photochromic behavior of spiropyrans allows for a deeper exploration of the electronic structure and solvent-dependent shifts in absorption spectra. While previous research has often focused on practical applications such as sensors or molecular switches, the intrinsic electronic interactions in these hybrid systems remain less understood. By focusing on the solvatochromic responses, this work aims to elucidate the role of solvent polarity and coordination effects on the electronic properties and stability of these complexes. Such a study not only contributes to the broader understanding of photo-responsive materials but also lays the groundwork

Scheme 1 Representation of the reaction of lanthanide nitrate ions and SPCOOH (MC isomer) to form LnMC complexes

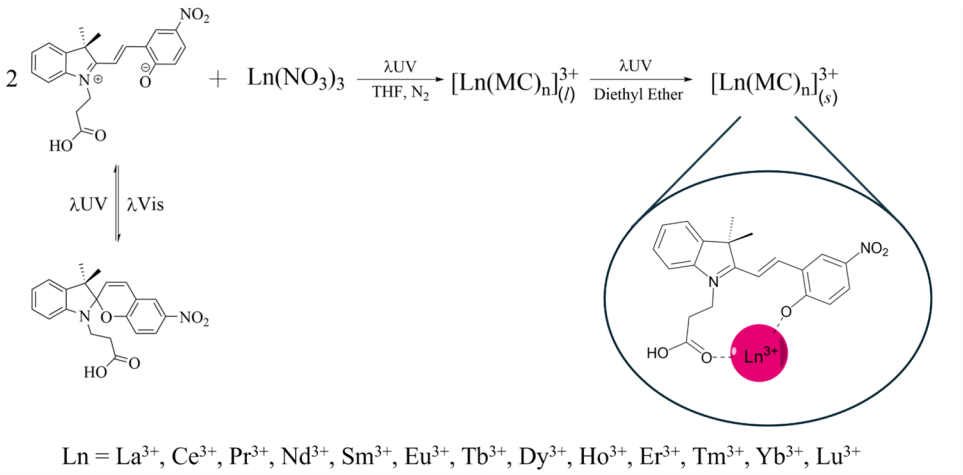

Ln = La^{3+}, Ce^{3+}, Pr^{3+}, Nd^{3+}, Sm^{3+}, Eu^{3+}, Tb^{3+}, Dy^{3+}, Ho^{3+}, Er^{3+}, Tm^{3+}, Yb^{3+}, Lu^{3+}

for future applications by revealing key structure–property relationships.

Herein, we report the synthesis of 14 new complexes using the spiropyran derivative a N-substituted 6-nitrobenzospiropyran (SPCOOH) as ligand, and all the elements of the lanthanide's series except for the Promethium. The new complexes called LnMC (independent of the number of coordinated MC molecules) were structurally characterized by Fourier transform infrared spectroscopy, Raman spectroscopy, and mass spectrometry. UV–visible spectroscopy was used for electronic analysis and for determining the complexes' stability in acetonitrile. The solvatochromism properties, besides their luminescence property, were investigated through the electronic emission spectroscopy technique varying the alcohol size chain.

Experimental

Reagents and solvents

The following reagents were acquired from Sigma-Aldrich: 2,3,3-trimethylindolenine (98%), 3-iodopropanoic acid (95%), 2-hidroxy-5-nitrobenzaldehyde (98%), 4-methylpiperidine (96%), tetrahydrofuran (THF) anhydrous (≥ 99.9%), Methanol (MeOH) (≥ 99.8%) and diethyl ether (Et_2O) anhydrous (≥ 99.0%), nitric acid (65%), 1-Propanol (≥ 99.5%), 1-butanol (≥ 99.5%) and 1-octanol (≥ 99.5)% from Quimex, acetonitrile (MeCN) (> 99.5%) from Synth, the Ln_2O_3 acquired from STARM were used to prepare the $Ln(NO_3)_3$ salt using HNO_3 65% (Quimex) (see procedure in Supporting Information-SI 1).

Ligand and coordination complex synthesis

The spiropyran (SPCOOH) molecule, (l-(β-Carboxyethyl)-3′,3′-dimethyl-6-nitrospiro (indoline-2′,2[2H-1] benzopyran), was synthesized following the literature procedure (Fissi et al. 1995). The Ln^{3+} complexes with SPCOOH (LnMC) were synthesized using a molar ratio of 2:1 (ligand: metal) according to our previous works (Reis et al. 2020; Miguez et al. 2019, 2020), and its synthesis is presented in Scheme 1. Briefly, SPCOOH was solubilized in anhydrous THF and kept under UV radiation (at 365 nm) for 15 min, followed by the addition of Ln^{3+} salts (previously solubilized in anhydrous THF). Immediately following the Ln^{3+} addition into the SPCOOH solution, a color change was observed from purple to dark red/orange, accordingly with the lanthanide salt added. The reaction was kept for 1 h, at room temperature, under UV radiation (at 365 nm), and N_2 atmosphere. The solid-state complexes (red or orange powders) were obtained from the precipitation of its THF solution in anhydrous Et_2O induced by UV light irradiation at 365 nm.

Structural characterization of LnMC

FTIR analyses were obtained using a PerkinElmer Spectrum 100 instrument equipped with a diamond crystal ATR module (wavelength range 650–4000 cm^{-1}; 4 cm^{-1} resolution; 64 scans) for the complexes LnMC and the ligand SPCOOH. Raman spectra were obtained using a RFS 100 FT-Raman Bruker spectrophotometer equipped with a germanium detector, liquid nitrogen cooling, and a 1064 nm NdYAG laser for excitation. Samples were placed on small aluminum holders, and scattered radiation was collected at a 180 ° angle. An average of 256 scans was performed to acquire each spectrum, with a resolution of 4 cm^{-1} within the range of 4000–400 cm^{-1}.

For the mass spectrometry, the experiments were conducted using a 6530 Accurate-Mass Q-TOF system with a Dual AJS ESI source and a 1260 Infinity II high-performance liquid chromatography instrument, both from Agilent

Technologies. The room temperature was maintained at 23 °C through air conditioning, and humidity levels were monitored (56–60%). Mass calibration and system cleaning were performed before analyses. Mobile phase cleaning runs were conducted, and each sample (10.0 µL) was directly injected into the high-performance liquid chromatograph (HPLC) system. Data were collected in positive ESI mode, scanning from m/z 100 to 2000 at 1 spectrum/sec scan rate, with capillary voltage at + 3.5 kV and fragmentor voltage at + 10 V. Nebulizer pressure, drying gas, and sheath gas were set at specified conditions for optimal performance.

Electronic characterization of LnMC

Absorption spectra were measured in the UV–visible range (from 200 to 800 nm) using a Varian Cary 50 Scan spectrophotometer and quartz cuvettes with a path length of 10 mm and volume of 1.5 mL. The photochromism of SPCOOH and the LnMC complexes were evaluated by UV–visible measurements using MeCN at 1×10^{-4} mol L^{-1}. The LnMC complexes' stability in MeCN solution was also investigated (10^{-5} mol L^{-1}). Then, kinetics studies were carried out using the UV–visible spectrophotometer, in which the analyses were conducted over a total duration of 16 h, with spectra taken every minute for the first hour and every 5 min thereafter. A quartz cuvette of 1 mL with a Teflon cap was used for the analyses in the absence of external visible radiation during the analysis. UV–visible spectra using methanol, 1-propanol, 1-butanol, and 1-octanol were obtained, as well as to conduct a solvatochromic study for the LnMC complexes. All UV–visible studies were conducted in the dark, at room temperature (20 ± 1 °C).

Emission spectra in MeCN diluted solution (10^{-5} mol L^{-1}) were recorded in a spectrofluorophotometer model Shimadzu RF-5301PC, with a xenon lamp as an excitation source. The RFPC software equipment control was used, to select an excitation wavelength at 460 nm, with excitation and emission, slits at 3, and slow scanning speed. Solution preparation and experimental handling were performed under controlled light intensity.

Results and discussion

Structural characterization of LnMC complex

The LnMC complexes were characterized using FTIR-ATR analysis, to get insights about their structures. Then, a comparison between the SPCOOH and the GdMC complex spectra (Fig. 1a) was carried out in the solid state.

Upon comparing both spectra, subtle variations are observed in the bands. Specifically, minor variations are discernible concerning the bands associated with the -OH stretching for the hydration water and the carboxyl acid molecules (see Figure SI 1). However, upon closer examination of the bands associated with the C=O stretching, notable differences are detected. In the GdMC complex, as an example, this band is situated at 1588 cm^{-1}, while in the SPCOOH ligand, it manifests at 1710 cm^{-1}. This clear distinction, characterized as a bathochromic shift, is indicative of the complexation reaction taking place (Miguez et al. 2019, 2020). These two shifts in the –OH and C=O bands suggest the coordination of the metal ion by both binding sites (Miguez et al. 2024; Sylvia et al. 2018). A similar phenomenon is observable, albeit with lower shifts, with

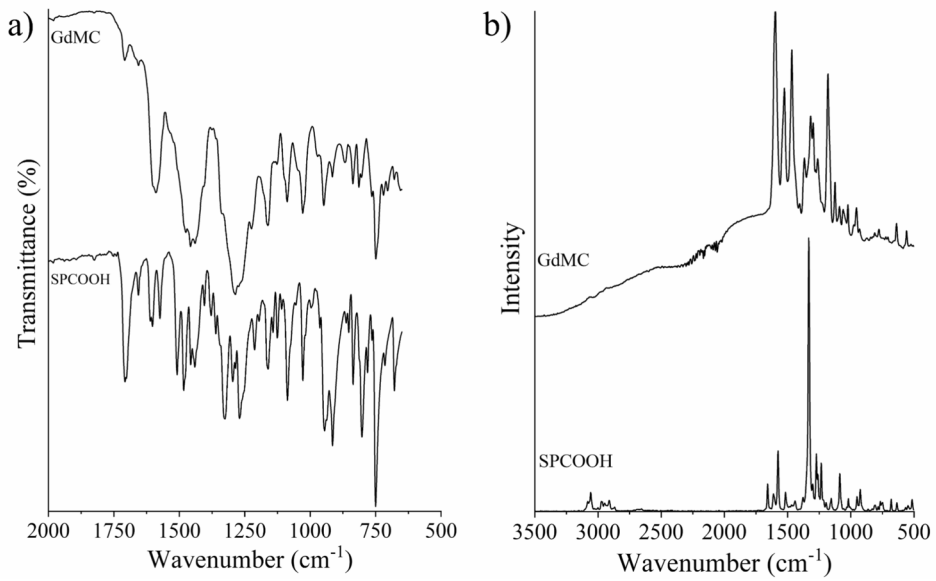

Fig. 1 **a** FTIR-ATR spectra of SPCOOH and GdMC complex. **b** Raman spectra of SPCOOH and GdMC complex

bands that correspond to the $–NO_2$ asymmetric and $–NO_2$ symmetric stretching, with values of 1483 and 1328 cm^{-1} for the ligand and 1447 and 1286 cm^{-1} for the complex, respectively. Additionally, in lower wavenumbers, bands indicate the presence of two and four aromatic hydrogen atoms within the cycle, with values of 802 and 749 cm^{-1} for the ligand and 811 and 745 cm^{-1} for the complex. Notably, the spiropyran ligand exhibits distinct bands at 1234 and 1091 cm^{-1}, related to asymmetric and symmetric stretches of the C–O–C ether bonds (De Sousa et al. 2010; F. Reis et al. 2020; Miguez et al. 2019, 2020), which is not present in the complex's spectrum. The observed bathochromic shift, coupled with the emergence of a secondary band as a shoulder adjacent to the C–O band of the complex (attributed in this context to phenolate), suggests coordination by lanthanide metals (Ln^{3+}) at these sites. This inference gains support from subsequent mass analysis confirming the presence of two and three ligands coordinated with the metal ions. Similar analyses can be extended to other complexes, as indicated by the minor variations observed in the bands discussed earlier. These findings are summarized in Table SI 1 and Figure SI 1.

To support these findings, Raman spectroscopy was performed, and the spectra for both the ligand and the GdMC complex can be found in (Fig. 1b); spectra for remaining complexes are presented in Figure SI 1. Comparing the spectra, one initially observes a band in the 3200–2800 cm^{-1} region, which corresponds to the C-H stretching from the sp^2 carbon in the H–C=C–H group of the SPCOOH ligand; this band is missing in the complex's spectrum due to its lower resolution. Additionally, a notable bathochromic shift in the band associated with C=O stretching, moving from 1660 cm^{-1} in the ligand to 1595 cm^{-1} in the complex, suggests a complexation reaction (Mcmillan & Hofmeister 1996). Based on this solid-state analysis, Scheme 1 represents the binding coordination of a MC isomer to the metal ion.

Mass analyses were carried out to validate the formation of coordination compounds and to identify the chemical species formed from the chemical reaction in the solution. Table 1 presents the most relevant peaks identified for each complex (see Figure SI 2 for all spectra), which were correlated with their respective molecular formulas. Based on these data, it is possible to verify that not only one complex can be obtained from the precipitation method used. However, the molecular formulas found can be correlated with other data previously observed in the literature. After analyzing all the peak values presented in Table 1, it is noticeable that in all cases there is the presence of the molecular ion peak, with values ranging from 898 to 934 m/*z*, corresponding to the general formula $[Ln(MC)_2]^{3+}$. Similar results have been reported in the literature with the same spiropyran derivative, involving ions such as Zn^{2+}, Co^{2+}, and also La^{3+} and Eu^{3+} (Reis et al. 2020; Miguez et al. 2019, 2020; Netto et al. 2024), as well as with other spiropyran derivatives coordinated to different metal ions (Baldrighi et al. 2016; Feuerstein et al. 2019; Liu et al. 2022). In addition, a ratio of 3:1 ligand to metal ion was verified for the La^{3+}, Sm^{3+}, Ho^{3+}, and Lu^{3+} ions; these structures are probably observed due to the metal ion radius. Similarly, data were observed for Ca^{2+} ion reported by Feuerstein et al. (2019).

Table 1 Values of molecular ion peaks observed for LnMC complexes

Complexes	$[Ln(MC)_2]^{3+}$	$[Ln(MC)_3]^{3+}$	$[Ln(MC)_3(H_2O)]^{3+}$	$[Ln(MC)_3(H_2O)_2]^{3+}$	$[Ln(MC)_3(NO_3)]^{2+}$
LaMC	898.29 *(899.18)*	1279.11 *(1279.32)*	1299.28 *(1297.33)*	–	1341.31 *(1341.31)*
CeMC	900.71 *900.18*	–	–	–	–
PrMC	900.38 *(900.98)*	–	1301.37 *(1303.42)*	–	–
NdMC	904.77 *(902.18)*	–	–	–	–
SmMC	912.26 *(912.19)*	1293.33 *(1292.33)*	1311.92 *(1310.34)*	1329.90 *(1328.35)*	–
EuMC	913.22 *(913.20)*	1291.79 *(1293.33)*	1311.34 *(1311.34)*	–	–
GdMC	918.20 *(918.20)*	1298.24 *(1298.34)*	1316.39 *(1316.35)*	–	–
TbMC	917.02 *(919.20)*	1297.10 *(1299.34)*	1319.00 *(1317.35)*	–	–
DyMC	922.23 *(924.20)*	1304.12 *(1304.34)*	1322.29 *(1322.35)*	–	–
HoMC	924.05 *(925.200*	1304.43 *(1305.34)*	1322.88 *(1323.35)*	1341.69 *(1341.36)*	–
ErMC	925.94 *(926.20)*	–	–	–	–
TmMC	929.66 *(929.20)*	–	1329.18 *(1327.36)*	–	–
YbMC	934.61 *(934.21)*	–	1332.50 *(1332.36)*	–	–
LuMC	934.18 *(935.22)*	1314.33 *(1315.35)*	1335.40 *(1333.36)*	1349.30 *(1351.37)*	–

(in italic) the calculated values

Electronic properties for the LnMC complex

The UV–vis and emission spectroscopies were employed to obtain information about electronic transitions for the LnMC complexes in solution. The UV–vis spectra for the GdMC complex under UV radiation (on) and under visible light radiation (off), as well as for the spiropyrans isomers (SP and MC), are presented in Fig. 2a.

Analyzing the spectra presented in Fig. 2a, a hypsochromic shift of 93 nm is observed comparing the bands in the visible region for the black spectrum (GdMC—on) to the orange spectrum (MC isomer). This shift indicates complex formation, corroborating the infrared and Raman analysis results. When comparing the spectra for the complex irradiated with UV or visible radiation, the absence of a band in the visible region for the red spectrum (GdMC—off) indicates the ligand dissociation of the complex and formation of the SP isomer, which does not coordinate with metal ions (Keyvan Rad et al. 2022; Kumar and Kumar 2020; Sylvia et al. 2018). The bands observed in the UV region for both spiropyran (SPCOOH) molecule and the GdMC—off complex is originated from electronic transitions in the indole region of the SPCOOH molecule (Tyer and Becker 1970). Data for the other complex are presented in Figure SI 3, and the hypsochromic shifts of the bands in the visible region for all complexes are listed in Table 2.

Figure 2b displays the emission spectra obtained for all 14 complexes. Although the emission bands of Ln^{3+} ions are distributed across different spectral regions and are characteristically narrow (Zinna and Di Bari 2015), the studied complexes show similar band profiles in terms of width and region. The λ_{max} values ranged from 560 to 578 nm; however, most complexes had their maximum emission at 565 nm, with LaMC, CeMC, and NdMC complexes displaying some variation. Previous studies reported similar band profiles with λ_{max} at 594, 566, and 600 nm in solution, for complexes containing the same spiropyran derivative with Zn^{2+} Eu^{3+}, and La^{3+}, respectively (Reis et al. 2020; Miguez et al. 2020; Netto et al. 2024). Although the studied cations belong to the same series (lanthanides) and have electrons in f orbitals, these ions differ in their ionic radius and electronic transitions. Their coordination to spiropyran derivatives can

Table 2 Maximum wavelength (λ_{max} in nm) for the LnMC complexes at visible spectrum region and $\Delta\lambda_{max} = \lambda_{max}$ LnMC—λ_{max} SPCOOH. All spectra were obtained in MeCN

Complexes	λ_{max} LnMC (nm)	$\Delta\lambda_{max}$ (nm)
LaMC	465	97
CeMC	477	85
PrMC	476	86
NdMC	474	88
SmMC	470	92
EuMC	478	84
GdMC	469	93
TbMC	471	91
DyMC	479	83
HoMC	465	97
ErMC	470	92
TmMC	464	98
YbMC	466	96
LuMC	463	99

λ_{max} SPCOOH at 562 nm

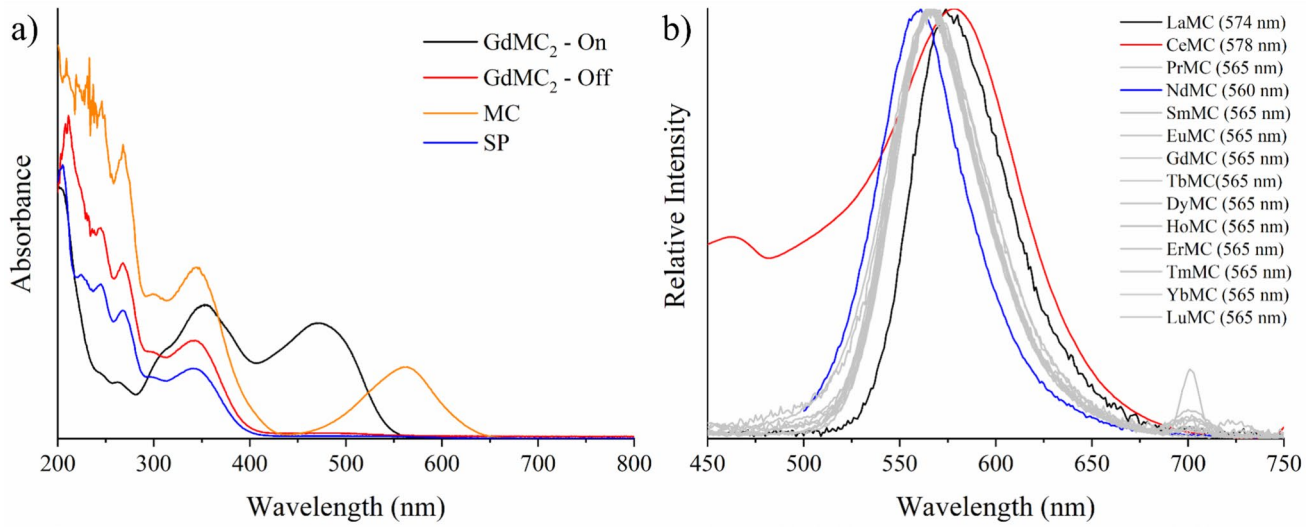

Fig. 2 **a** UV–vis spectra for the GdMC complex (on and off), SP, and MC. **b** Emission spectrum for all complexes studied. All spectra were obtained in MeCN

lead to variations in the absorption spectra, including using the SPCOOH. However, this effect appears to be less pronounced in emission for the coordination complexes between the lanthanides and the SPCOOH, suggesting that the spiropyran ligand (SPCOOH) is primarily responsible for this characteristic emission, independently of the metal ion.

To qualitatively investigate the complexes' stability in solution, UV–vis experiments were carried out as a function of the time for all synthesized complexes using MeCN as solvent. Previous studies (Miguez et al. 2020; Ozhogin et al. 2019, 2023) have highlighted the enhanced stability of the spiropyran ligands and their coordination complex in this solvent. Upon analyzing all the spectra shown in Figure SI 4, data presented for these 14 complexes demonstrated a greater stability over time for the coordination complexes formed by the following ions: La^{3+}, Ce^{3+}, Sm^{3+}, Gd^{3+}, Tb^{3+}, Ho^{3+}, Tm^{3+}, and Yb^{3+}. A common observation across all the complexes spectra is in no case the absorbance reaches zero, suggesting that the LnMC complex is predominant in solution, compared to the dissociated species (Ln^{3+} ion and SPCOOH ligand). However, due to the dissociation of part of the complex, an equilibrium between coordinated MC and free SP is present in the solution, which is supported by reports showing that with no radiation influence, there is a portion of MC in solution formed by solvent interactions given its solvatochromic properties (Liu et al. 2022; Tian and Tian 2014).

Solvatochromic properties

Spiropyran derivatives are also well known for its ability to interact in different ways when exposed to different solvents; these changes are traditionally associated with a few parameters such as solvent polarity and hydrogen bonding interactions (Liu et al. 2022; Tian and Tian 2014). In addition to the solvatochromic behavior of the SPCOOH (MC isomer) in methanol, 1-propanol, 1-butanol, and 1-octanol, this property was also investigated for all 14 complexes using the same solvents. Although the solvatochromism for spiropyran derivatives has been reported in the literature, there are few data for the coordination complexes using these organic molecules as ligand. Figure SI 5 depicts the absorption spectra for these complexes and for the ligand (SPCOOH) in methanol, 1-propanol, 1-butanol, and 1-octanol. Table SI 2 detailed the corresponding λ_{max} for all samples in the visible region.

Initially, the SPCOOH ligand (in its MC isomer form) displayed vivid colors in all four tested alcohols, ranging from red in methanol to purple in 1-octanol. After 12 h without exposure to UV or visible light, the MC isomer was partially stabilized in methanol, 1-propanol, and 1-octanol. This behavior aligns with previous literature (Abdollahi et al. 2017; Menzonatto and Lopes 2022), which reports that protic solvents stabilize the MC isomer of spiropyran derivatives due to hydrogen bonding between solvent and solute. Following irradiation with visible light, the SP isomer was restored, confirming the reversible nature of the isomerization process. Figure 3 illustrates the relationship between the maximum absorption wavelength and the lanthanide ion for all 14 complexes.

Upon analyzing the results for methanol, 1-propanol, 1-butanol, and 1-octanol, a decreasing trend in wavelength values was observed with increasing atomic number of the metal center across the series. In methanol (Fig. 3a), the maximum absorption in the visible range varied from 486 to 503 nm, although the correlation with the lanthanide electronic configuration was weak ($R^2 = 0.33$). However, in 1-propanol (Fig. 3b), a stronger linear correlation was observed between the electronic configuration of the lanthanides and the λ_{max} ($R^2 = 0.94$), suggesting a greater degree of hydrogen bonding between the solvent and solute (LnMC complexes). As the alcohol chain length increased, the correlation weakened, with R^2 values of 0.67 in 1-butanol and 0.76 in 1-octanol (Fig. 3c and 3d). Since no correlation was verified for each LnMC coordination complex with solvent polarity, the hydrogen bond interaction could be related to these λ_{max} variation.

Conclusion

This study offers a detailed examination of the synthesis, structural characterization, and electronic properties of novel lanthanide complexes (LnMC) derived from a spiropyran ligand (SPCOOH). The successful synthesis, confirmed through techniques like FTIR-ATR, Raman spectroscopy, and mass spectrometry, highlights the effective complexation between lanthanide ions and the ligand. The electronic characterization, using UV–visible and emission spectroscopy, reveals significant shifts in absorbance and emission profiles, further confirming complex formation and demonstrating stability in acetonitrile, which underscores their potential, not limited to the solvatochromic applications. The observed solvatochromic and electronic transition (absorption and emission) properties of these complexes open promising avenues for further research, particularly in the development of advanced materials for optical and electronic devices. Future studies could explore interactions with other solvents and ions or examine their behavior in

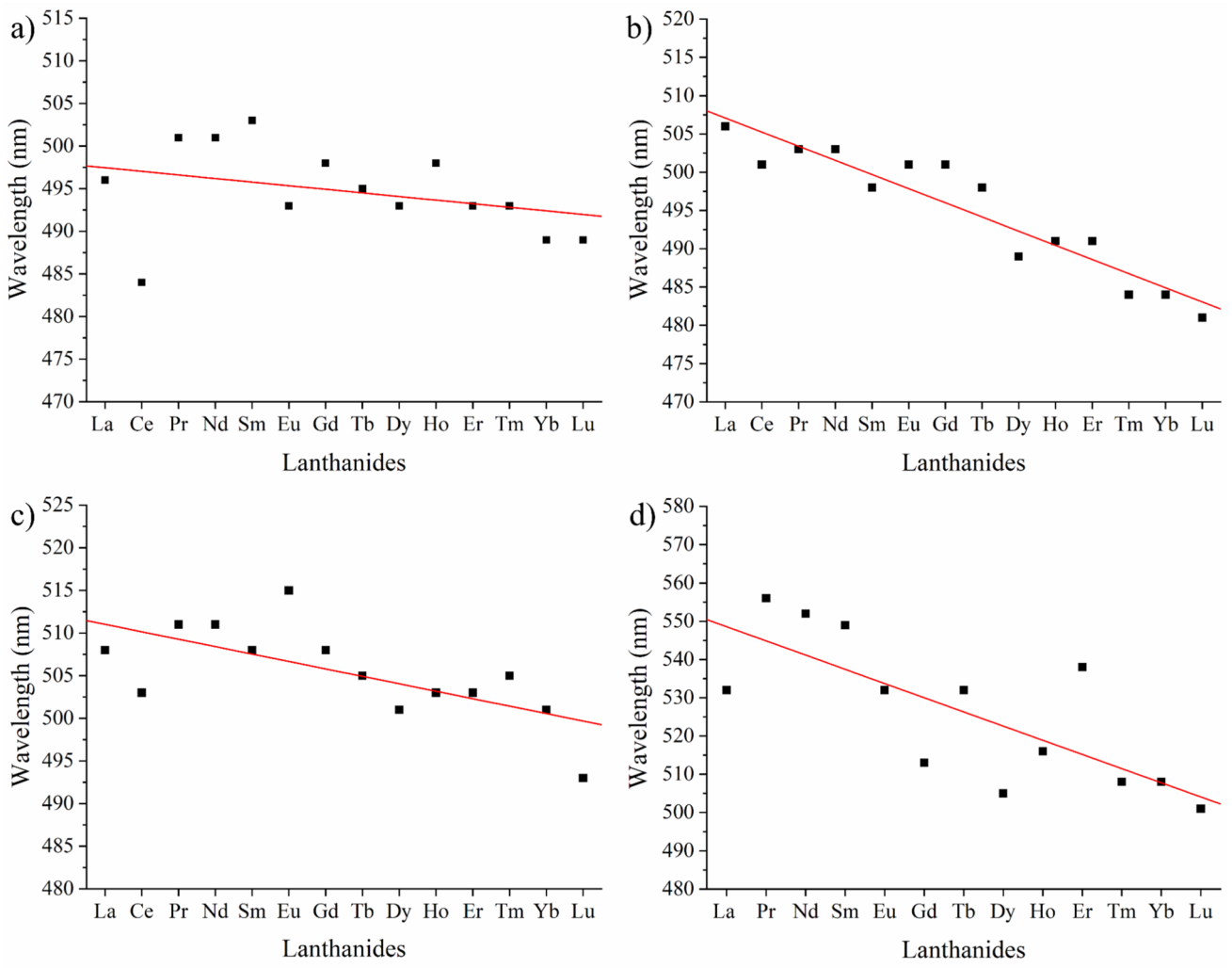

Fig. 3 Relationship between maximum wavelength (λ_{max}) values observed in the spectra of LnMC complexes for: **a** methanol ($R^2 = 0.33$), **b** 1-propanol ($R^2 = 0.94$), **c** 1-butanol ($R^2 = 0.67$), and **d**1-octanol ($R^2 = 0.76$)

varied environmental conditions. This work enriches the understanding of lanthanide-sensitized materials, providing a strong foundation for future research and practical applications in the field of chemistry.

Supplementary Information The online version contains supplementary material available at https://doi.org/10.1007/s11696-025-03990-0.

Acknowledgements This work was supported by CNPq (grant numbers 406853/2021-5, 303569/2022-0, and also scholarship 140243/2021-6), FAPEMIG (grant numbers APQ-00210-21, APQ-04537-22, RED-00045-23, APQ-03079-23, and APQ-00144-24), and FINEP (0187/22 - INFRASPEC). This work was also supported by Doaplex Tecnologia, Pesquisa e Desenvolvimento S.A. agreement with UNIFEI (process number 23088.014641/2021-67) which made the DAI/CNPq 2020 agreement possible.

Declarations

Conflict of interest The authors declare that they have no conflict of interest.

References

Abdel-Mottaleb MSA, Saif M, Attia MS, Abo-Aly MM, Mobarez SN (2018) Lanthanide complexes of spiropyran photoswitch and sensor: spectroscopic investigations and computational modelling. Photochem Photobiol Sci 17(2):221–230. https://doi.org/10.1039/c7pp00226b

Abdollahi A, Alinejad Z, Mahdavian AR (2017) Facile and fast photosensing of polarity by stimuli-responsive materials based on spiropyran for reusable sensors : a physico-chemical study on the interactions. J Mater Chem C 5:6588–6600. https://doi.org/10.1039/c7tc02232h

Attia MS, Khalil MMH, Abdel-Mottaleb MSA, Lukyanova MB, Alekseenko YA, Lukyanov B (2006) Effect of complexation with lanthanide metal ions on the photochromism of (1,3,3-trimethyl-5′-hydroxy-6′-formyl-indoline-spiro2,2′-[2h] chromene) in different media. Int J Photoenergy 2006:1–9. https://doi.org/10.1155/IJP/2006/42846

Baldrighi M, Locatelli G, Desper J, Aakeröy CB, Giordani S (2016) Probing metal ion complexation of ligands with multiple metal binding sites: the case of spiropyrans. Chem Eur J 22(39):13976–13984. https://doi.org/10.1002/chem.201602608

Bao G, Wen S, Lin G, Yuan J, Lin J, Wong KL, Bünzli JCG, Jin D (2021) Learning from lanthanide complexes: the development of dye-lanthanide nanoparticles and their biomedical applications. Coord Chem Rev 429:213642. https://doi.org/10.1016/j.ccr.2020.213642

Chen X, Liu Y, Tu D (2014) Lanthanide-doped luminescent nanomaterials. Springer, Berlin Heidelberg. https://doi.org/10.1007/978-3-642-40364-4

Danylchuk DI, Jouard PH, Klymchenko AS (2021) Targeted solvatochromic fluorescent probes for imaging lipid order in organelles under oxidative and mechanical stress. J Am Chem Soc 143(2):912–924. https://doi.org/10.1021/jacs.0c10972

De Sousa FB, Guerreiro JDT, Ma M, Anderson DG, Drum CL, Sinisterra RD, Langer R (2010) Photo-response behavior of electrospun nanofibers based on spiropyran-cyclodextrin modified polymer. J Mater Chem 20(44):9910–9917. https://doi.org/10.1039/c0jm01903h

Feuerstein TJ, Müller R, Barner-Kowollik C, Roesky PW (2019) Investigating the photochemistry of spiropyran metal complexes with online LED-NMR. Inorg Chem 58(22):15479–15486. https://doi.org/10.1021/acs.inorgchem.9b02547

Fissi A, Pieroni O, Ruggeri G, Ciardelli F (1995) Photoresponsive polymers. Photomodulation of the macromolecular structure in poly(L-lysine) containing spiropyran units. Macromolecules 28(1):302–309. https://doi.org/10.1021/ma00105a042

Florea L, McKeon A, Diamond D, Benito-Lopez F (2013) Spiropyran polymeric microcapillary coatings for photodetection of solvent polarity. Langmuir 29(8):2790–2797. https://doi.org/10.1021/la304985p

Gao M, Shen B, Zhou J, Kapre R, Louie AY, Shaw JT (2020) Synthesis and comparative evaluation of photoswitchable magnetic resonance imaging contrast agents. ACS Omega 5(24):14759–14766. https://doi.org/10.1021/acsomega.0c01534

Homocianu M (2024) Exploring solvatochromism: a comprehensive analysis of research data. Microchem J 198:110166. https://doi.org/10.1016/j.microc.2024.110166

Hur DY, Shin EJ (2015) Solvatochromic and photochromic behavior of spiropyran-cored PAMAM dendron and Cu^{2+}-selective sensing. Bull Korean Chem Soc 36(1):104–110. https://doi.org/10.1002/bkcs.10027

Keyvan Rad J, Balzade Z, Mahdavian AR (2022) Spiropyran-based advanced photoswitchable materials: a fascinating pathway to the future stimuli-responsive devices. J Photochem Photobiol C Photochem Rev 51:100487. https://doi.org/10.1016/j.jphotochemrev.2022.100487

Klajn R (2014) Spiropyran-based dynamic materials. Chem Soc Rev 43(1):148–184. https://doi.org/10.1039/C3CS60181A

Kortekaas L, Browne WR (2019) The evolution of spiropyran: fundamentals and progress of an extraordinarily versatile photochrome. Chem Soc Rev 48(12):3406–3424. https://doi.org/10.1039/c9cs00203k

Kozlenko AS, Ozhogin IV, Pugachev AD, Lukyanova MB, El-Sewify IM, Lukyanov BS (2023) A modern look at spiropyrans: from single molecules to smart materials. Top Curr Chem 381(1):8. https://doi.org/10.1007/s41061-022-00417-2

Kumar A, Kumar S (2020) A benzothiazolinic spiropyran for highly selective, sensitive and visible light controlled detection of copper ions in aqueous solution. J Photochem Photobiol A Chem 390:112265. https://doi.org/10.1016/j.jphotochem.2019.112265

Liu G, Li Y, Cui C, Wang M, Gao H, Gao J, Wang J (2022) Solvatochromic spiropyran—a facile method for visualized, sensitive and selective response of lead (Pb^{2+}) ions in aqueous solution. J Photochem Photobiol, A 424:113658. https://doi.org/10.1016/j.jphotochem.2021.113658

Mcmillan PF and Hofmeister AM (1996) Infrared and Raman spectroscopy. In: Handbook of Grignard reagents, CRC Press, pp 121–130. https://doi.org/10.1201/b16932-10

Menzonatto TG, Lopes JF (2022) The role of intramolecular interactions on the stability of the conformers of a spiropyran derivative. Chem Phys 562:111654. https://doi.org/10.1016/j.chemphys.2022.111654

Miguez FB, Reis IF, Dutra LP, Silva IMS, Verano-Braga T, Lopes JF, De Sousa FB (2019) Electronic investigation of light-induced reversible coordination of Co(II)/spiropyran complex. Dyes Pigm 171:107757. https://doi.org/10.1016/j.dyepig.2019.107757

Miguez FB, Menzonatto TG, Netto JFZ, Silva IMS, Verano-Braga T, Lopes JF, De Sousa FB (2020) Photo-dynamic and fluorescent zinc complex based on spiropyran ligand. J Mol Struct 1211:128105. https://doi.org/10.1016/j.molstruc.2020.128105

Miguez FB, Trigueiro JPC, Lula I, Moraes ES, Atvars TDZ, de Oliveira LFC, Alexis F, Nobuyasu RS, De Sousa FB (2024) Photochromic sensing of La^{3+} and Lu^{3+} ions using poly(caprolactone) fibers doped with spiropyran dyes. J Photochem Photobiol, A 452:115568. https://doi.org/10.1016/j.jphotochem.2024.115568

Morimoto M, Takagi Y, Hioki K, Nagasaka T, Sotome H, Ito S, Miyasaka H, Irie M (2018) A turn-on mode fluorescent diarylethene: Solvatochromism of fluorescence. Dyes Pigm 153(February):144–149. https://doi.org/10.1016/j.dyepig.2018.02.016

Netto JFZ, Miguez FB, Bahia SBBB, Bolais-Ramos LG, Verano-Braga T, Trigueiro JPC, Nobuyasu RS, Brandão TAS, De Sousa FB (2024) Core-sheath organic-inorganic hybrid electrospun fibers for organophosphorus heterogeneous catalysis. J Environ Chem Eng 12(5):113267. https://doi.org/10.1016/j.jece.2024.113267

Ozhogin IV, Chernyavina VV, Lukyanov BS, Malay VI, Rostovtseva IA, Makarova NI, Tkachev VV, Lukyanova MB, Metelitsa AV, Aldoshin SM (2019) Synthesis and study of new photochromic spiropyrans modified with carboxylic and aldehyde substituents. J Mol Struct 1196:409–416. https://doi.org/10.1016/j.molstruc.2019.06.094

Ozhogin IV, Pugachev AD, Kozlenko AS, Rostovtseva IA, Makarova NI, Borodkin GS, El-Sewify IM, Metelitsa AV, Lukyanov BS (2023) Methyl 5′-Chloro-8-formyl-5-hydroxy-1′,3′,3′-trimethylspiro-[chromene-2,2′-indoline]-6-carboxylate. Molbank 2023(1):M1549. https://doi.org/10.3390/M1549

Pandey N, Tewari N, Pant S, Mehata MS (2022) Solvatochromism and estimation of ground and excited state dipole moments of 6-aminoquinoline. Spectrochim Acta Part A Mol Biomol Spectrosc 267:120498. https://doi.org/10.1016/j.saa.2021.120498

Reis F, Miguez FB, Vargas CAA, Menzonatto TG, Silva IMS, Verano-Braga T, Lopes JF, Brandão TAS, De Sousa FB (2020) Structural and electronic characterization of a photoresponsive lanthanum(III) complex incorporated into electrospun fibers for phosphate ester catalysis. ACS Appl Mater Interfaces 12(25):28607–28615. https://doi.org/10.1021/acsami.0c03571

Rocha J, Carlos LD, Paz FAA, Ananias D (2011) Luminescent multifunctional lanthanides-based metal–organic frameworks. Chem Soc Rev 40(2):926–940. https://doi.org/10.1039/C0CS00130A

Selvanathan P, Huang G, Guizouarn T, Roisnel T, Fernandez-Garcia G, Totti F, Le Guennic B, Calvez G, Bernot K, Norel L, Rigaut S (2016) Highly axial magnetic anisotropy in a

N3O5Dysprosium(III) coordination environment generated by a merocyanine ligand. Chem Eur J 22(43):15222–15226. https://doi.org/10.1002/chem.201603439

Stock RI, Nandi LG, Nicoleti CR, Schramm ADS, Meller SL, Heying RS, Coimbra DF, Andriani KF, Caramori GF, Bortoluzzi AJ, Machado VG (2015) Synthesis and Solvatochromism of Substituted 4-(Nitrostyryl)phenolate dyes. J Org Chem 80(16):7971–7983. https://doi.org/10.1021/acs.joc.5b00983

Sylvia GM, Mak AM, Heng S, Bachhuka A, Ebendorff-Heidepriem H, Abell AD (2018) A rationally designed spiropyran-based chemosensor for magnesium. Chemosensors 6(2):17. https://doi.org/10.3390/chemosensors6020017

Tian W, Tian J (2014) An insight into the solvent effect on photo-, solvato-chromism of spiropyran through the perspective of intermolecular interactions. Dyes Pigm 105:66–74. https://doi.org/10.1016/j.dyepig.2014.01.020

Tyer NW, Becker RS (1970) Photochromic spiropyrans. I. Absorption spectra and evaluation of the .pi.-electron orthogonality of the constituent halves. J Am Chem Soc 92(5):1289–1294. https://doi.org/10.1021/ja00708a031

Wang M, Liu G, Gao H, Su C, Gao J (2023) Preparation and performance of reversible thermochromic phase change microcapsules based on negative photochromic spiropyran. Colloids Surf A Physicochem Eng Asp 659:130808. https://doi.org/10.1016/j.colsurfa.2022.130808

Zhang S, Zhang Q, Ye B, Li X, Zhang X, Deng Y (2009) Photochromism of spiropyran in ionic liquids: enhanced fluorescence and delayed thermal reversion. J Phys Chem B 113(17):6012–6019. https://doi.org/10.1021/jp9004218

Zinna F, Di Bari L (2015) Lanthanide circularly polarized luminescence: bases and applications. Chirality 27(1):1–13. https://doi.org/10.1002/chir.22382

Authors and Affiliations

Jorge Fernandes Z. Netto[1] · Flávio B. Miguez[1] · Nathália E. N. Mendonça[1] · Olívia B. O. Moreira[2] · Marcone A. L. de Oliveira[2] · Luiz F. C. de Oliveira[3] · Roberto S. Nobuyasu[4] · Frederico B. De Sousa[1]

✉ Frederico B. De Sousa
fredbsousa@gmail.com; fredbsousa@unifei.edu.br

[1] Laboratório de Sistemas Poliméricos e Supramoleculares (LSPS), Instituto de Física e Química, Universidade Federal de Itajubá (UNIFEI), Itajubá, MG 37500-903, Brazil

[2] Grupo de Química Analítica e Quimiometria (GQAQ), Departamento de Química - ICE, Universidade Federal de Juiz de Fora (UFJF), Juiz de Fora, MG 36036-900, Brazil

[3] Núcleo de Espectroscopia e Estrutura Molecular, Departamento de Química - ICE, Universidade Federal de Juiz de Fora (UFJF), Juiz de Fora, MG 36036-900, Brazil

[4] Laboratório de Fotofísica - Instituto de Física e Química, Universidade Federal de Itajubá (UNIFEI), Itajubá, MG 37500-903, Brazil